Electronic Supplementary Information

Photoresponsive Spiropyran-Functionalised MOF-808: Postsynthetic Incorporation and Light Dependent Gas Adsorption Properties

Katherine Healey,[a] Weibin Liang,[a] Peter D. Southon,[a] Tamara L. Church,[a,] and Deanna M. D'Alessandro[a*]

[a] School of Chemistry, The University of Sydney, Sydney, New South Wales 2006, Australia.

Corresponding author email: deanna.dalessandro@sydney.edu.au

S1 Syntheses

All chemicals and solvents were purchased from commercial sources and used as received without further purification.

S1.1 *1-(carboxymethyl)-2,3,3,-trimethyl-3H-indol-1-ium iodide* (P) Synthesis

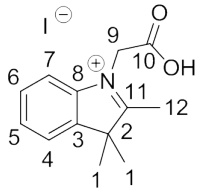

P was synthesised according to a procedure modified from the synthesis of 1-(2-carboxyethyl)-2,3,3,-trimethylindolenium iodide.[1] 2,3,3-Trimethylindolenine (3.22 g, 20.0 mmol) was added to iodoacetic acid (3.73 g, 20.0 mmol) under N_2 with stirring. The dark red solution was then vigorously stirred at 40 °C until the solution solidified, and was then heated for 3 hours at 80 °C to give a dark red solid. The solid was dissolved in water and washed with chloroform (5 × 50 mL). The aqueous layer was collected and evaporated under reduced pressure to give a yellow residue. This was dissolved in a minimum amount of acetone and reprecipitated from ether (100 mL). A yellow powder was isolated by filtration and washed with ether (2 × 50 mL) (2.67 g, 39 %). ^{1}H NMR (500 MHz, d_6-dmso): δ 7.91 (s, 1H, **H4**), 7.85 (s, 1H, **H5**), 7.61 (s, 2H, **H5**, **H6**), 5.50 (s, 2H, **H9**), 2.81 (s, 3H, **H12**), 1.56 (s, 6H, **H1**) ppm. ^{13}C{^{1}H} NMR (125 MHz, d_6-dmso): δ 166.3 (**C10**), 141.2 (**C3**, **C8**), 129.5 (**C5**), 129.1 (**C7**), 115.1 (**C4**), 54.3 (**C11**), 48.8 (**C9**), 29.7 (**C2**), 22.1 (**C1**), 14.4 (**C12**) ppm. Elemental Analysis: Found C, 45.42; H, 4.50; N, 3.96 %; Calculated for $C_{13}H_{16}INO_2$: C, 45.24; H, 4.67; N, 4.06 %. ESI-MS (ESI$^+$, MeOH): 218.01 (Calculated $[M–I]^+$ = 218.12, 100 %) amu.

S1.2 MOF-808 syntheses

MOF-808 ($[Zr_6O_4(OH)_4(btc)_2(HCOO)_6]$ was synthesised according to the literature procedures.[2, 3] The experimental XRPD, FTIR and ^{1}H NMR data were consistent with those reported.[2, 3]

S1.3 Postsynthesis modification of MOF-808

$[Zr_6O_4(OH)_4(btc)_2(HCOO)_{6-n}(P)_n]$ (MOF-808-P) was synthesised by appendage of P onto the Zr_6 cluster in MOF-808. P (0.148 mg, 0.420 mmol) was added to a suspension of MOF-808 (397 mg, 0.420 mmol) in DMF (10 mL) in a 21-mL vial. The solution was left to sit overnight at room temperature. The product was then washed sequentially with DMF (3 × 25 mL), acetone (5 × 25 mL) and ethanol (5 × 25 mL) and dried *in vacuo* to yield a pink powder (4% based on P). Elemental Analysis: Found C, 20.30; H, 3.05; N, 1.19%; Calculated for $[Zr_6O_4(OH)_4(btc)_2(HCOO)_{5.95}(P)_{0.05}]\cdot 0.12DMF\cdot 8.2H_2O\cdot 0.65(C_2H_5OH)$: C, 20.30; H, 3.05; N, 0.93%.

$[Zr_6O_4(OH)_4(btc)_2(HCOO)_{6-n}(P)_{n-x}(SP)_x]$ (MOF-808-SP) was synthesised by functionalisation of P after appendage on to the Zr_6 nodes in MOF-808. MOF-808-P (139 mg,

0.101 mmol) was suspended in butanone (1 mL). Piperidine (12.5 μL, 0.130 mmol) was added and the suspension was refluxed at 60 °C for 10 minutes. 2-Hydroxy-5-nitrobenzaldehyde (25.0 mg, 151 μmol) was dissolved in a minimum amount of butanone (*ca.* 0.5 mL) and added to the reaction. The solution was then heated with stirring at 60 °C for 5 minutes and left to stand overnight at room temperature. The resulting product was then washed with acetone (10 × 25 mL) and ethanol (10 × 25 mL) to yield an orange-red powder (50% based on P). Elemental Analysis: Found C, 23.71; H, 3.23; N, 1.08%; Calculated for $[Zr_6O_4(OH)_4(btc)_2(HCOO)_{5.95}(P)_{0.03}(SP)_{0.02}]\cdot 0.12DMF\cdot 3H_2O\cdot 2.9(C_2H_5OH)$: C, 23.71; H, 3.23; N, 0.93 %.

The maximum theoretical amount of spiropyran that could be incorporated, was estimated by considering the relative sizes of MOF-808 pores, and the spiropyran. The cavity size in MOF-808 is 16.6 Å, such that the theoretical ratio of spiropyran (~14.9 x 8.5 x 7 Å)[4] incorporation is 1 spiropyran per pore. Since one Zr_6 cluster has 6 formates pointing into 6 different pore windows, and since one cavity is constructed from 12 Zr_6 clusters, it follows that that the maximum amount of spioropyran that could be incorporated would be 1 spiropyran for every 2 Zr_6 clusters.

S2 Nuclear Magnetic Resonance (NMR)

^1H and $^{13}C\{1H\}$ NMR spectra were obtained on a Bruker AVANCE300 or 500 spectrometer operating at 300 or 500 MHz for ^1H and at 75 or 125 MHz for ^{13}C. Spectra were recorded at 298 K and chemical shifts (δ) were referenced internally to residual deuterated solvent signals with an uncertainty of ± 0.01 Hz and ± 0.05 Hz for ^1H and ^{13}C, respectively. Coupling constants (*J*) are reported with an uncertainty of ± 0.05 Hz. Approximately 5 mg of product was dissolved in a deuterated solvent as specified. ^1H NMR spectra of digested MOFs were obtained by decomposing the materials in KOH/D_2O and filtering the solution through Celite prior to measurement.

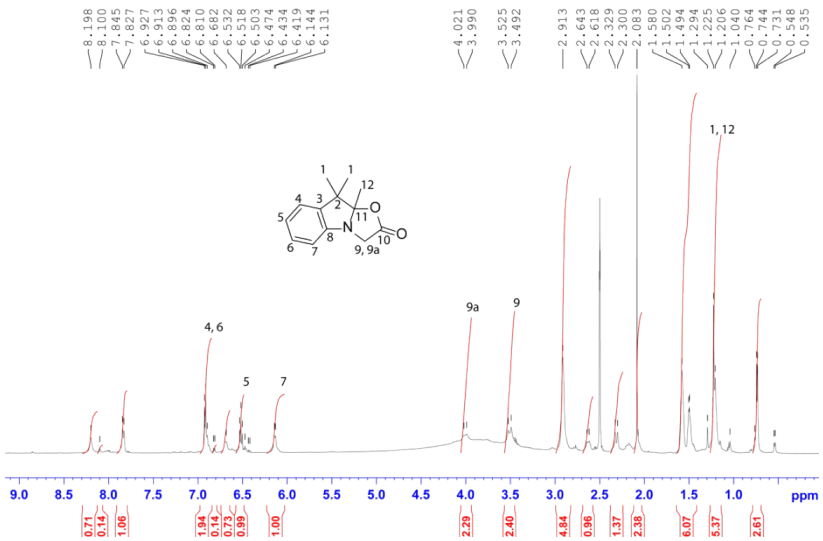

Fig. S1 ^{1}H NMR of 9,9,9a-trimethyl-9,9a-dihydrooxazolo[3,2-a]indol-2(3*H*)-one (cyclic P).

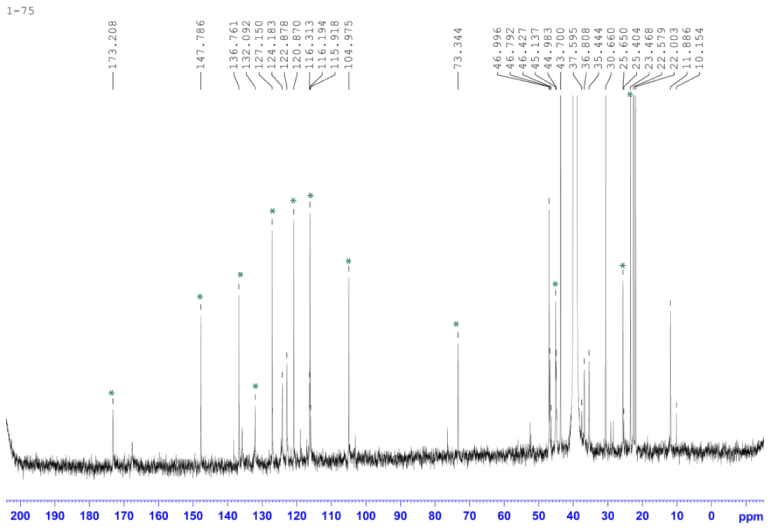

Fig. S2 ^{13}C{^{1}H} NMR of cyclic P with the peaks assigned (*) (One quaternary carbon was not observed).

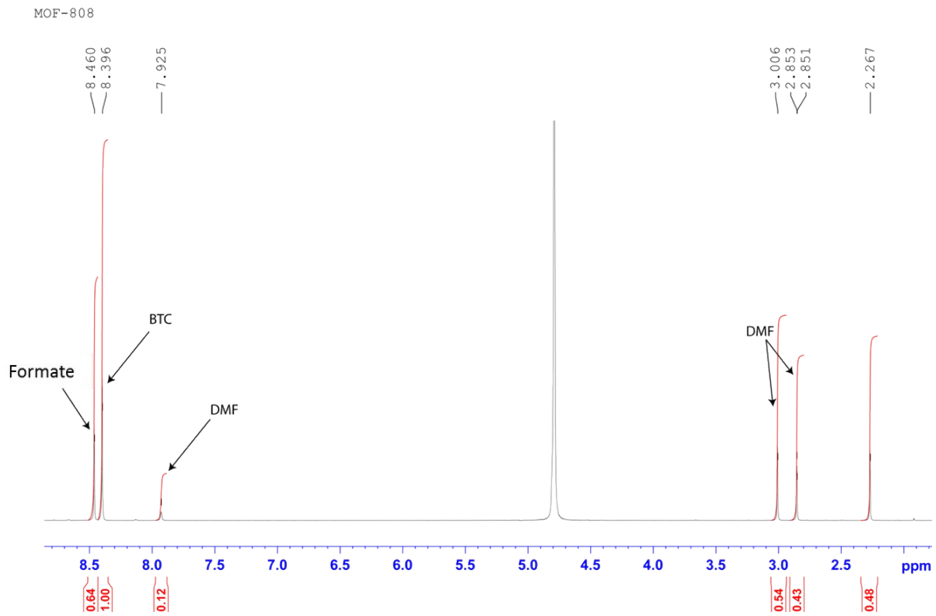

Fig. S3 ^{1}H NMR of alkaline-digested (KOH/D_2O) MOF-808.

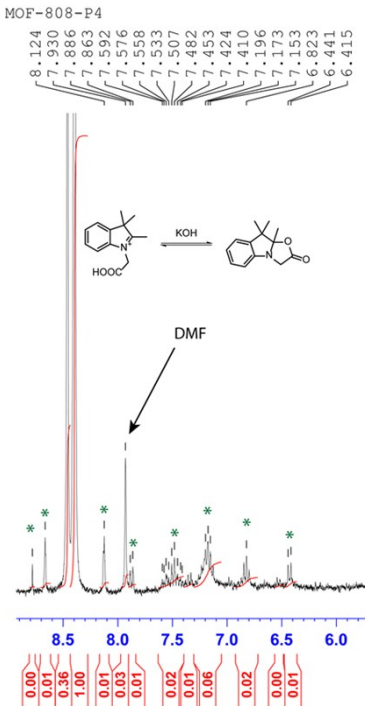

Fig. S4 ^{1}H NMR of alkaline-digested (KOH/D_2O) MOF-808-P showing peaks characteristic of P (*).

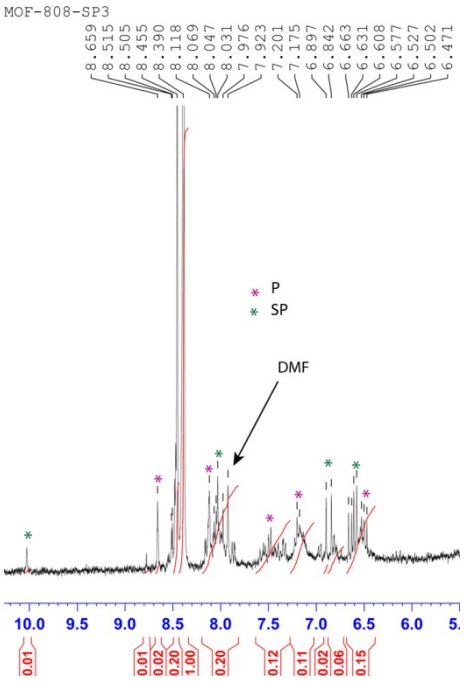

Fig. S5 ^{1}H NMR of alkaline-digested (KOH/D_2O) MOF-808-SP showing peaks characteristic of P (purple) and SP (green).

S3 Ultraviolet (UV) Studies

UV studies were conducted after irradiating each sample for 30 min at 254 nm using a 230 V Spectroline UV lamp (40 W).

S4 X-ray Powder diffraction (XRPD)

XRPD patterns were obtained using a PANalytical X'Pert PRO Diffractometer. A Cu anode was used to produce K_α radiation ($\lambda_{K\alpha}$ = 1.54056 Å). Flat plate diffraction data was collected for the range 2θ = 5–50 ° with a step size of 0.02 ° and a scan rate of 2 ° s^{-1}. Profile fits were performed using the Le Bail extraction method in GSAS.

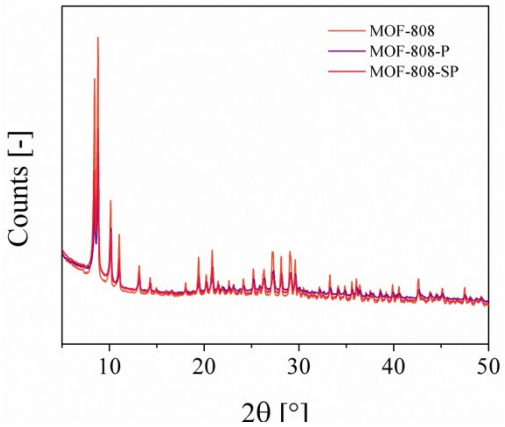

Fig. S6 XRPD patterns of MOF-808 (orange), MOF-808-P (purple), and MOF-808-SP (pink).

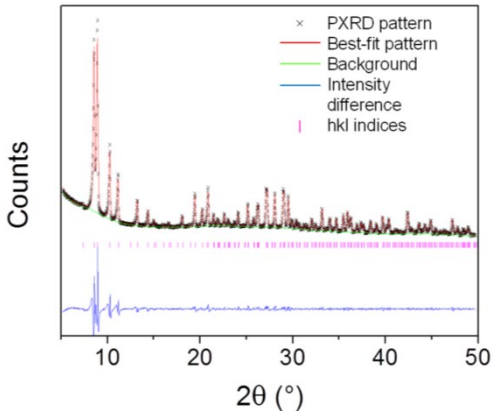

Fig. S7 *Le Bail* refinement of MOF-808, showing the experimental (black), refined (red), and difference (blue) patterns. The positions of the Bragg peaks are indicated by the pink bars.

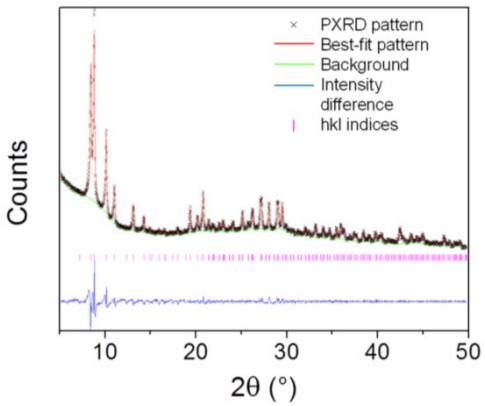

Fig. S8 *Le Bail* refinement of MOF-808-P, showing the experimental (black), refined (red), and difference (blue) patterns. The positions of the Bragg peaks are indicated by the pink bars.

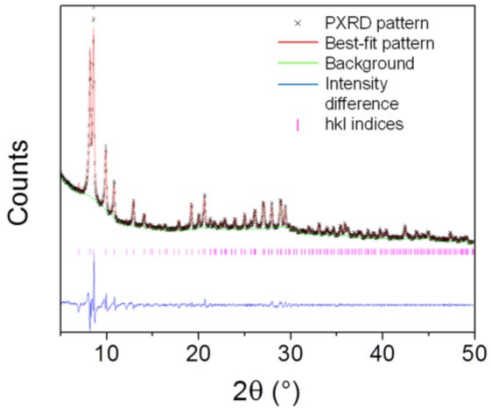

Fig. S9 *Le Bail* refinement of MOF-808-SP, showing the experimental (black), refined (red), and difference (blue) patterns. The positions of the Bragg peaks are indicated by the pink bars.

S5 Thermogravimetric analysis (TGA)

TGA data was collected on a Discovery Thermogravimetric Analyser. Approximately 3–

5 mg of sample was placed on a platinum pan and heated from room temperature to 700 °C at a rate of 3 °C min^{-1}. Each sample was heated under a constant flow of *ca.* 0.1 L min^{-1} N_2.

For the aerobic TGA curves of MOF-808, MOF-808-P, and MOF-808-SP (Figures S10 - S12), the first weight loss (up to ~60 °C) is consistent with solvent removal from the framework pores. From ~60 to 700 °C, the organic components in MOF-808, MOF-808-P, and MOF-808-SP gradually decompose, with ZrO_2 as the remaining material at 700 °C.

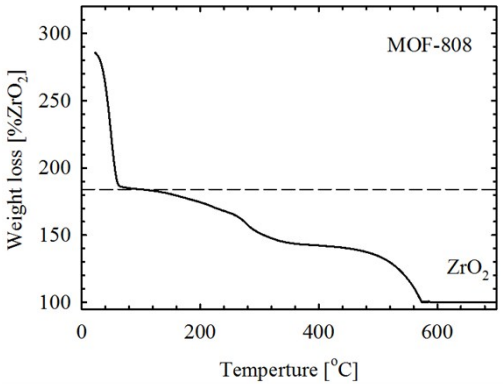

	Formula	Molecular weight
MOF-808	$[Zr_6O_4(OH)_4(C_9H_3O_6)_2(CHO_2)_6]$	1363.344

Fig. S10 Thermogravimetric analysis (TGA) showing the weight loss (related to ZrO_2). Black dashed line indicates the theoretical weight for activated MOF-808.

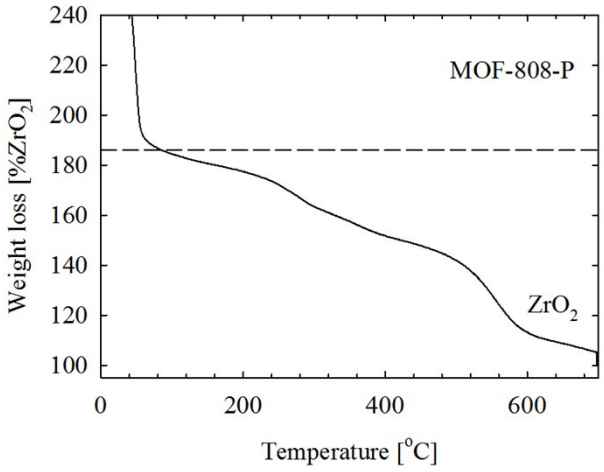

	Formula	Molecular weight
MOF-808-P	$[Zr_6O_4(OH)_4(C_9H_3O_6)_2(CHO_2)_{5.95}(C_{13}H_{16}NO_2I)_{0.05}]$	1378.339

Fig. 11 Thermogravimetric analysis (TGA) showing the weight loss (related to ZrO_2). Black dashed line indicates the weight loss for activated MOF-808-P.

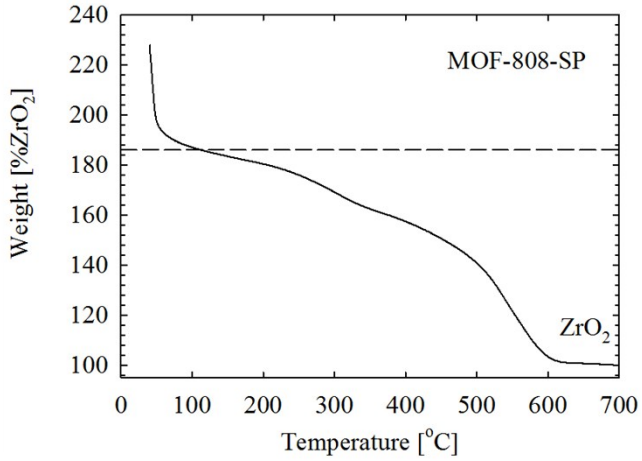

	Formula	Molecular weight
MOF-808-P	$[Zr_6O_4(OH)_4(C_9H_3O_6)_2(CHO_2)_{5.95}$ $(C_{13}H_{16}NO_2I)_{0.03}(C_{20}H_{17}N_2O_5)_{0.02}]$	1378.741

Fig. S12 Thermogravimetric analysis (TGA) showing the weight loss (related to ZrO_2). Black dashed line indicates the weight loss for activated MOF-808-SP.

S6 Fourier Transform Infrared (FTIR) spectroscopy

FTIR spectra of ligands and MOFs were obtained on a PerkinElmer UATR Two Spectrometer using approximately 0.5 mg of a ground sample. 16 scans were recorded over the range of 400–4000 cm^{-1}.

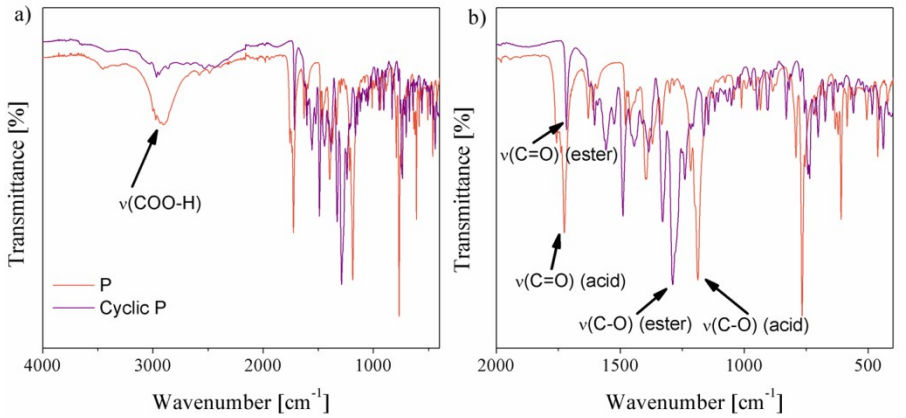

Fig. 13 Solid state FTIR spectra of P (orange) and cyclic P (purple) with a) showing the full scale and b) showing the fingerprint region.

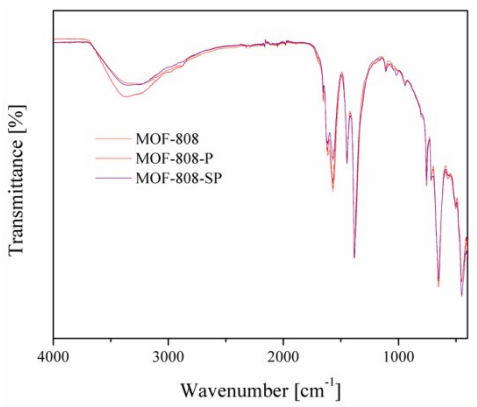

Fig. S14 Solid state FTIR spectra of MOF-808 (orange), MOF-808-P (pink) and MOF-808-SP (purple).

S7 Mass Spectrometry

Mass spectrometry measurements were carried out on a Bruker amaZon SL mass spectrometer. Approximately 1 µg of sample was dissolved in HPLC grade methanol and ionised by electrospray ionisation.

S8 Solid state Ultra Violet-Visible-Near Infrared (UV-vis-NIR) Spectroscopy

Solid state UV-vis-NIR spectroscopy was completed using a CARY5000 UV-vis-NIR Spectrophotometer with a Praying Mantis™ attachment by scanning between 5000–50000 cm^{-1} with a scan rate of 6000 cm^{-1} min^{-1}. Approximately 5 mg of sample was ground in 50 mg of $BaSO_4$, which was used for baseline correction. Variable temperature (VT) data was collected using the Praying Mantis™ High Temperature Reaction Chamber from 30–100 °C at a ramp rate of 0.5 °C min^{-1}. Data was collected every five minutes over the range 12500–50000 cm^{-1} with a scan rate of 10000 cm^{-1} min^{-1}.

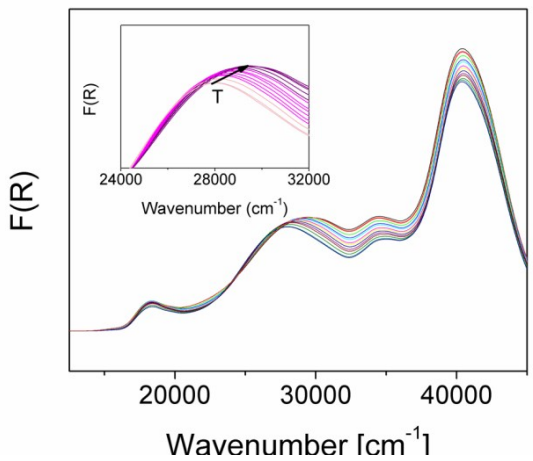

Fig. S15 Variable temperature (VT) UV-vis spectra of UV-irradiated MOF-808-SP. VT data was collected from 30–100 °C at a ramp rate of 0.5 °C min^{-1}.

S9 Gas Sorption

Adsorption isotherms were obtained on a Micromeritics 3Flex Surface Characterisation

Analyser. Approximately 80 mg of sample was placed into a glass analysis tube and degassed under vacuum for 12 h at 100 °C prior to measurement.

S9.1 Surface Area

Argon (Ar) adsorption and desorption isotherms were measured at 87 K. The isotherms were then analysed to determine the Brunauer–Emmet–Teller (BET) surface area using the MicroActive software (Version 3.00, Micromeritics Instrument Corp. 2013).

S9.2 Pore size distribution

The pore size distributions were determined by analysing the Ar isotherms using the cyclindrical density functional theory (DFT) model for Ar on oxides at 87 K.

S9.3 UV irradiated gas sorption

Samples were loaded into a quartz NMR tubes and evacuated overnight, heated to 100 °C for 12 h, and finally exposed to UV light for 30 min. The NMR tubes were then placed in glass 3Flex tubes that were backfilled with N_2 and analysed as described above.

S9.4 CO_2 and heat of adsorption measurements

The CO_2 heat of adsorption was determined by comparing the CO_2 adsorption isotherms at 298, 308, and 318 K. The data was fitted using the Clausius–Clapeyron equation (eq. S1) to calculate the isosteric heat of adsorption (Q_{st}):

$$(lnP)_n = -\left(\frac{Q_{st}}{R}\right)\left(\frac{1}{T}\right) + C \qquad \text{eq. S1}$$

where P is pressure, n is amount adsorbed, T is temperature, R is the universal gas constant and C is a constant.

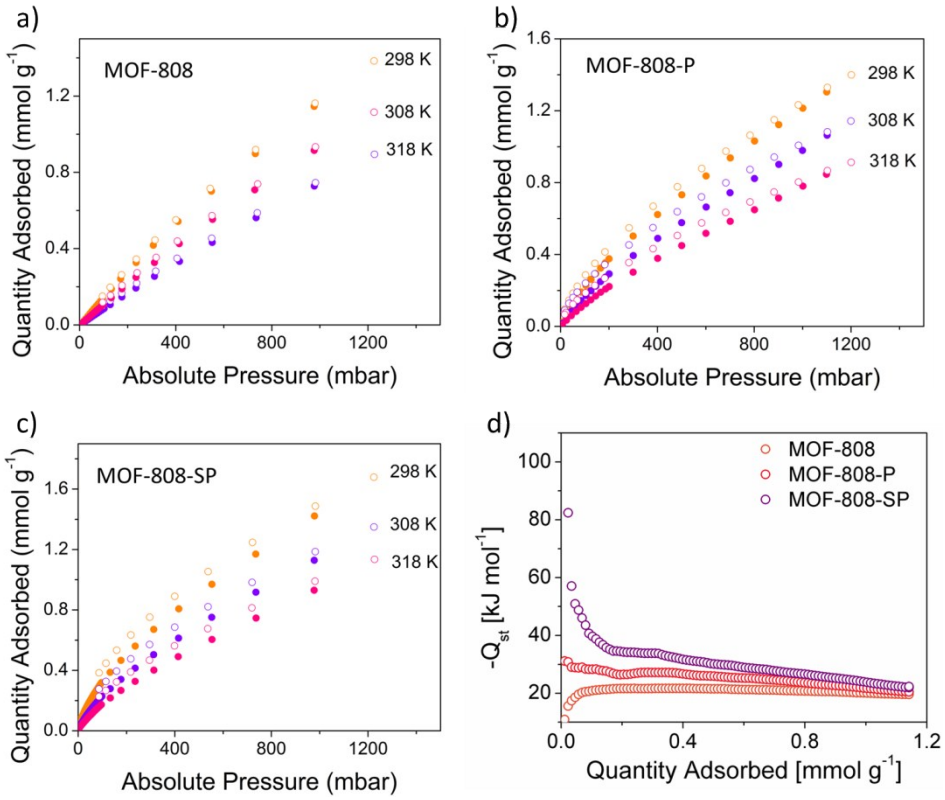

Fig. S16 CO_2 uptake at 298, 308, and 318 K for MOF-808 (a), MOF-808-P (b), and MOF-808-SP (c) as well as isosteric heat of CO_2 adsorption profiles (d) for MOF-808 (orange), MOF-808-P (red), and MOF-808-SP (purple).

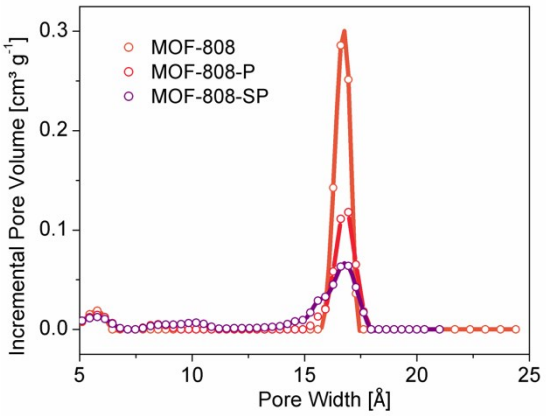

Fig. S17 Pore size distributions for MOF-808 (orange), MOF-808-P (red), and MOF-808-SP (purple).

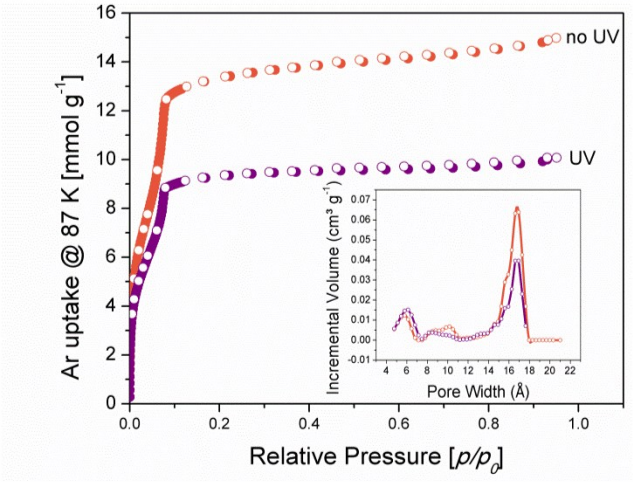

Fig. S18 Ar sorption isotherms and pore size distribution profiles (inset) for MOF-808-SP before (orange) and after UV irradiation (purple).

S10 Elemental Analysis

Elemental analyses were performed at the Chemical Analysis Facility at Macquarie University. Each sample was evacuated at room temperature prior to analysis. Two values for each element were obtained.

S11 References

1. X. Li, Y. Wang and T. Matsuura, J. Meng, *Heterocycles*, 1999, **51**, 2639-2651.
2. W. Liang, H. Chevreau, F. Ragon, P. D. Southon, V. K. Peterson and D. M. D'Alessandro, *CrystEngComm*, 2014, **16**, 6530-6533.
3. H. Furukawa, F. Gándara, Y.-B. Zhang, J. Jiang, W. L. Queen, M. R. Hudson and O. M. Yaghi, *J. Am. Chem. Soc.*, 2014, **136**, 4369-4381.
4. F. Zhang, X. Zou, W. Feng, X. Zhao, X. Jing, F. Sun, H. Ren and G. Zhu, J. *Mater. Chem*., 2012, **22**, 25019-25026.